Comprehensive Conformational Analysis of the Four- to Twelve-Membered Ring Cycloalkanes: Identification of the Complete Set of Interconversion Pathways on the MM2 Potential Energy Hypersurface

István Kolossváry*,† and Wayne C. Guida

Contribution from the Research Department, Pharmaceuticals Division, CIBA-GEIGY Corporation, Summit, New Jersey 07901. *Received June 16, 1992*

Abstract: Comprehensive conformational analysis of the 4- to 12-membered ring hydrocarbon series cyclobutane through cyclododecane has been carried out. The complete set of minima and saddle points has been located on the MM2 potential energy hypersurface using systematic and Monte Carlo conformational search techniques associated with a combination of Newton-type energy minimization methods. The complete network of conformational interconversions has also been identified. It has been found that the different modes of conformational interconversion associated with the lowest barriers between minimum energy conformers display fascinating patterns of well-coordinated atomic movement.

Introduction

Cyclic hydrocarbons have long been a major target of conformational analysis.[1a] The basic concepts of conformational interconversion between symmetrical conformers of small- and medium-ring hydrocarbons have long been perpetuated in the organic chemistry literature where conformational interconversions have been described, for example, by considering the so-called pseudorotational itinerary. In fact, pseudorotation is the fundamental concept that has been used to explain ring puckering in cyclopentane.[2] Pseudorotation is also the mode of interconversion between the different twist-boat forms of cyclohexane as well as between different symmetrical conformers of larger ring hydrocarbons. Pseudorotation usually surmounts low-energy barriers and is associated with a simultaneous change of all ring torsion angles without severe distortions in bond angles. During pseudorotation, ring symmetry is broken; namely, a ring form with a plane of symmetry pseudorotates into another form with an axis of symmetry and vice versa. Another mode of conformational interconversion, the so-called symmetrical mode, retains symmetry. However, this mode usually crosses higher energy barriers than pseudorotation and is associated with high torsional strain as well as severe distortion of bond angles localized to a ring bond triplet.[3] Well-known examples of the symmetrical mode are transitions from the cyclohexane chair form to the twist-boat form retaining an axis of symmetry, and to the boat form retaining a plane of symmetry. All these concepts were developed in full detail by Hendrickson in a series of classical papers[4] where the familiar circular and globular diagrams of pseudorotation pathways used in numerous organic chemistry textbooks were first described.

Hendrickson pointed out that pseudorotation and the symmetrical mode of interconversion are concepts well-suited for symmetrical ring forms only.[4c] At that time only symmetrical ring forms were considered as the prime candidates for minima as well as transition states. Nonetheless, Hendrickson suggested the existence of asymmetrical modes of conformational interconversion in cyclooctane and other larger rings.[4c] It now seems evident that asymmetrical conformers and transition states are, in fact, quite common in medium- and large-ring hydrocarbons. Indeed, there are many potential asymmetrical modes of conformational interconversion in medium and large rings which exhibit a considerably lower energy barrier than any plausible symmetrical mode and/or pseudorotation.[5] Thus, if the goal of conformational analysis is a complete description of all low-energy minima and transition states, methodology unencumbered with bias imposed by symmetry constraints must be sought.

Early analyses of conformational interconversions in rings were based on chemical intuition supported by Dreiding models and molecular mechanics calculations. Although chemical intuition in good hands is a powerful tool, it is per se biased. Much of the bias has been eliminated by the Wiberg-Boyd "torsional driving" procedure[6] where one or more ring torsion angles are driven by small increments while simultaneously optimizing the geometry of the rest of the ring. A totally unbiased solution to the analysis of conformational interconversions is, however, based on the very successful concept of potential energy hypersurfaces.[7a,d] The potential energy hypersurface of a molecule accounts for all the symmetrical and asymmetrical minimum energy conformers and transition states. Minimum energy conformers correspond to local minima, and transition states correspond to saddle points on the potential energy hypersurface. Conformational interconversion pathways can also be defined in a strict mathematical manner based on the differential geometry description of potential energy hypersurfaces by Tachibana and Fukui.[8]

Recent developments in computational chemistry have made exploration of the potential energy hypersurface a practical reality. There is, however, a significant bias in contemporary conformational analysis. Maybe because it is more difficult to locate saddle points than local minima (see the Theory section), or maybe because the importance of saddle points has simply not been well appreciated, conformational analysis has been synonymous with a search for (low-energy) minima on the potential energy hypersurface. Although there has been a recent appreciation in the literature for the need of locating the (low-energy) saddle points

* Address correspondence to this author.
† Present address: Department of General and Analytical Chemistry, Technical University of Budapest, Szt. Gellért tér 4, 1111 Budapest, Hungary.

(1) Burkert, U.; Allinger, N. L. *Molecular Mechanics*; American Chemical Society: Washington, DC, 1982; and references therein: (a) pp 89-108; (b) pp 72-76; (c) pp 119-121; (d) pp 89-91; (e) pp 98, 99; (f) p 102; (g) pp 105, 106.

(2) Kilpatrick, J. E.; Pitzer, K. S.; Spitzer, R. *J. Am. Chem. Soc.* **1947**, *69*, 2483-2488.

(3) Hendrickson[4c] describes the symmetrical mode, e.g., the C-TB interconversion in cyclohexane where "most of the deformation occurs at one pair of bonds". Figure 7 shows the superimposed C and TB forms as well as the transition state and suggests that a bond triplet, rather than a pair of bonds, is involved in the interconversion.

(4) (a) Hendrickson, J. B. *J. Am. Chem. Soc.* **1961**, *83*, 4537-4547. (b) Hendrickson, J. B. *Ibid.* **1964**, *86*, 4854-4866. (c) Hendrickson, J. B. *Ibid.* **1967**, *89*, 7047-7061.

(5) (a) Anet, F. A. L. *Top. Curr. Chem.* **1974**, *45*, 169-220. (b) Dale, J. *Top. Stereochem.* **1976**, *9*, 199-270.

(6) Wiberg, K. B.; Boyd, R. H. *J. Am. Chem. Soc.* **1972**, *94*, 8426-8430.

(7) (a) Mezey, P. G. *Potential Energy Hypersurfaces*; Elsevier: Amsterdam-Oxford-New York-Tokyo, 1987; (b) pp 163-169; (c) pp 78-81. (d) Heidrich, D.; Kliesch, W.; Quapp, W. *Properties of Chemically Interesting Potential Energy Surfaces*; Springer: Berlin, 1991. (e) pp 7, 8, 107-122.

(8) Fukui, K. *J. Phys. Chem.* **1970**, *74*, 4161-4163. Tachibana, A.; Fukui, K. *Theor. Chim. Acta (Berlin)* **1978**, *49*, 321-347. Tachibana, A.; Fukui, K. *Ibid.* **1979**, *51*, 275-296. Fukui, K. *Acc. Chem. Res.* **1981**, *14*, 363-368.

0002-7863/93/1515-2107$04.00/0

as well,[9] few examples have appeared in the literature. Saunders presented a "random kick" method[10] which can be used to identify pairs of minimum energy conformers likely to interconvert without, however, identifying the interconnecting saddle point.

We believe that full understanding of conformational space requires identification of the complete network of conformational interconversions (NCI) within a thermodynamically feasible energy window. We propose that the basic units of the NCI are the directly interconnected minimum-saddle-minimum triads (MSM triads) which represent a single conformational interconversion. Careful study of the MSM triads allows one to learn about modes of conformational interconversion in an unbiased manner. Since it is relatively straightforward to find the pair of minima associated with a particular saddle point (see the Theory section), our primary goal has been to locate (low energy) saddle points rather than minima on the potential energy hypersurface.

Methods

Theory. Visual distinction between local minima and saddle points on a two-dimensional (potential energy) surface is rather trivial. Mathematical distinction, however, is far more difficult. Both local minima and saddle points are stationary points on the (any dimensional) potential energy hypersurface (i.e., locations on the hypersurface where the energy gradient vanishes). The energy gradient is the first derivative vector of the potential energy with respect to the nuclear coordinates. The difference between minima and saddle points can only be detected by considering the Hessian matrix. The Hessian matrix is the second derivative matrix of the potential energy. Minima and saddle points can be distinguished by local curvature properties of the potential energy hypersurface expressed in terms of the eigenvalues of the Hessian matrix. Local minima are associated with a positive definite Hessian matrix, i.e., one with exclusively positive eigenvalues[11a] (canonical curvatures) as opposed to saddle points associated with a Hessian matrix with exactly one negative eigenvalue. In other words, at local minima the potential energy is minimized with respect to all directions defined by the eigenvectors of the Hessian matrix (all degrees of freedom), whereas at saddle points the potential energy is minimized in all but one direction which is defined by the eigenvector associated with the negative eigenvalue of the Hessian matrix. In this direction the potential energy is at a maximum.

Extensive research has been conducted in order to devise algorithms that converge upon saddle points rather than local minima.[1b,7b,12] Despite considerable effort, saddle point search techniques are prone to miss their target and converge upon minima, if they converge at all! There seems to be a rather trivial reason for this. Even if everything else fails when searching for local minima on the potential energy hypersurface, there is a trivial objective to lower the energy in each successive step. No such "rule of thumb" applies when searching for saddle points. It would seem to be viable to devise some kind of constrained minimization technique that would take advantage of the structural difference between the Hessian matrix associated with minima and the Hessian matrix associated with saddle points, but there is none of which we are aware. In fact, there is only one simple "foolproof" technique that can be used to search for saddle points. The well-known full-matrix Newton–Raphson (FMNR) algorithm converges alike upon minima, saddle points, or multiple maxima (stationary points where the Hessian matrix has more than one negative eigenvalues). This means that, when minimization starts from within the "catchment region" of a saddle point, convergence to that saddle point is theoretically assured. So-called augmented Hessian methods have been devised to modify the original FMNR algorithm so that convergence upon saddle points becomes more efficient. Cerjan and Miller have shown that, by applying an appropriate shift parameter to the eigenvalues of the Hessian matrix,[13a,b] the FMNR algorithm is prone to converge upon saddle points even if minimization starts from within the "catchment region" of a local minimum. Recent developments of other augmented Hessian techniques and introduction of the so-called trust radius or trust region concept[13c-e] further improved the efficiency of saddle point searches. The trust region delimits the area around a point on the potential energy hypersurface where the second-order Taylor expansion of the potential energy function is a good approximation. Minimization steps are limited to within the current trust radius which is continuously updated at each iteration. An interesting technique, the so-called streambed (valley floor) walk algorithm, uses a non-Newton step wherever the (augmented) Newton step would jump out of the trust region, possibly destroying the smooth convergence.[13f] The streambed is mathematically defined by the so-called gradient extremals.[7e,13f] Gradient extremals are lines on the potential energy hypersurface along which the gradient norm (the length of the gradient vector) of the potential energy function is at a minimum (extremum) with respect to variations within the iso-energy (contour) *subspace*. Gradient extremals are unique lines connecting stationary points on potential energy hypersurfaces. The streambed walk algorithm utilizes the (augmented) Newton step if there is a saddle point within the trust region, i.e., when the Hessian matrix has the proper structure (exactly one negative eigenvalue). If no saddle point exists inside the trust region, then the gradient extremal point on the boundary of the trust region is used as the next iteration point. Another interesting algorithm seeks the transition state between a known reactant and a known product by minimizing the energy of the product subject to the constraint that the structure of the reactant and the product remain geometrically separated by a fixed distance. The transition state is approached by continuously reducing the distance constraint.[13g,h] These ideas have been primarily utilized in quantum chemistry program packages.[13e,14]

Although the previously described algorithms could well be of utility in conformational analyses on molecular mechanics potential energy hypersurfaces, they have never been tested in this environment. There is a fundamental difference between energy minimization in conformational analysis, and energy minimization, or rather maximization, in quantum chemical calculations of reaction mechanisms where these algorithms have found widespread use. In the former case conformational space is sampled by systematically or randomly generating a large number of starting structures. These usually severely distorted, high-energy molecular structures (particularly in the case of cyclic molecules) have to then be optimized in terms of going downhill on the potential energy hypersurface toward a local minimum, or as is our goal, toward a saddle point. In the latter case, reactant and product are usually known, and an appropriate uphill movement is sought toward the interconnecting saddle point(s).

Although the sophisticated saddle point search algorithms used successfully in quantum chemistry program packages may be of utility for the searches presented in this paper, our approach to searching for (low-energy) saddle points on the MM2 molecular

(9) Anet, F. A. L. *J. Am. Chem. Soc.* **1990**, *112*, 7172–7178.

(10) Saunders, M. *J. Comput. Chem.* **1991**, *12*, 645–663.

(11) (a) The Hessian matrix in Cartesian space, i.e., when the atomic coordinates in the potential energy function are simply the X, Y, Z coordinates of each atom, is 6-fold degenerate at stationary points on the potential energy hypersurface. This means that the $3N \times 3N$ Hessian matrix has six zero eigenvalues (five for linear molecules) corresponding to the three translational and three rotational degrees of freedom in the three-dimensional space in which the molecule is represented. For a detailed analysis of the degeneracy of the Hessian matrix, see: Kolossváry, I.; McMartin, C. *J. Math. Chem.* **1992**, *9*, 359–367, and ref 7d, pp 78–85. (b) Eckart, C. *Phys. Rev.* **1935**, *47*, 552–558.

(12) Poppinger, D. *Chem. Phys. Lett.* **1975**, *35*, 550–554. Simons, J.; Jørgensen, P.; Taylor, H.; Ozment, J. *J. Phys. Chem.* **1983**, *87*, 2745–2753. Bell, S.; Crighton, J. S. *J. Chem. Phys.* **1984**, *80*, 2464–2475. Jensen, F. *J. Am. Chem. Soc.* **1992**, *114*, 1596–1603.

(13) (a) Cerjan, C. J.; Miller, W. H. *J. Chem. Phys.* **1981**, *75*, 2800–2806. (b) Banerjee, A.; Adams, N.; Simons, J.; Shepard, R. *J. Phys. Chem.* **1985**, *89*, 52–57. (c) Jørgen Aa., H.; Jørgensen, P.; Helgaker, T. *J. Chem. Phys.* **1986**, *85*, 3917–3929. (d) Nichols, J.; Taylor, H.; Schmidt, P.; Simons, J. *Ibid.* **1990**, *92*, 340–346. (e) Culot, P.; Dive, G.; Nguyen, V. H.; Ghuysen, J. M. *Theor. Chim. Acta* **1992**, *82*, 189–205. (f) Jørgensen, P.; Jørgen, H.; Jensen, A.; Helgaker, T. *Ibid.* **1988**, *73*, 55–65. (g) Dewar, M. J. S.; Healy, E. F.; Stewart, J. J. P. *J. Chem. Soc., Faraday Trans. 2* **1984**, *80*, 227–233. (h) Cummins, P. L.; Gready, J. E. *J. Comput. Chem.* **1989**, *10*, 939–950.

(14) Baker, J. *J. Comput. Chem.* **1986**, *7*, 385–395. Baker, J. *Ibid.* **1992**, *13*, 240–253.

mechanics potential energy hypersurface is a "winning combination" of the original FMNR algorithm and the so-called truncated Newton conjugate gradient (TNCG) algorithm,[15] two minimization techniques that have been used for conformational searches in molecular mechanics program packages. The TNCG algorithm in our hands has proven to be by far the most effective energy minimization method. Note, however, that the TNCG algorithm alone hardly ever converges upon saddle points. The reason behind the choice of this combination is the following. The global minimum energy point on the potential energy hypersurface is obviously a minimum-type stationary point. As one opens an energy window above the global minimum, more and more stationary points can be located. First, the lowest energy local minima appear followed by a mixture of the lowest energy saddle points and some slightly higher energy minima. As the energy window opens further, the minimum- and saddle-type stationary points disappear, and a mixture of uninteresting higher order multiple maxima can be seen. This picture shows the general trend that the low-energy regions of the potential energy hypersurface are dominated by minima and saddle points, whereas higher order multiple maxima tend to be also higher in energy; simply, because minima are minimized in all degrees of freedom, saddle points are minimized in all but one degree of freedom, and higher order multiple maxima are minimized in fewer and fewer degrees of freedom. There is, of course, a significant overlap between the lowest energy region associated with low-energy minima and the higher energy region associated with low-energy saddle points. Therefore, we propose the following computational procedure for searching low-energy saddle points on the potential energy hypersurface. First, minimize a starting molecular structure with the TNCG algorithm until its energy is lowered to within a thermodynamically reasonable energy window above the (current) global minimum of the conformational search. An alternative to this procedure is to minimize the starting structure with the TNCG algorithm to a reasonably low-energy gradient. Switch then to the FMNR algorithm which further lowers (or occasionally raises) the energy until full convergence is reached predominantly at either a saddle point or a local minimum.

This procedure works well in theory. In practice, however, problems arise with the FMNR algorithm. The FMNR algorithm produces at each iteration a displacement vector, the so-called FMNR step, which is used to move the atoms of the molecule to their new (usually lower energy) position. The displacement vector is the product of the negative energy gradient vector and the inverse Hessian matrix. It is well known that the full FMNR step often causes the molecule to "blow up" unless the minimization is very close to convergence. Even close to convergence, the FMNR algorithm is prone to oscillatory behavior.[9] Using sophisticated augmented Hessian methods with (updated) trust radius seems to have completely removed the difficulties arising with FMNR minimizations; however, there are even simpler remedies to help stabilize the FMNR algorithm. One procedure is to conduct a (quadratic) line search along the displacement vector for an energy minimum point. It is instructive to note that the line search procedure often fails to find a minimum energy point. There seems to be, however, a rather trivial trick that we have used successfully to rectify this situation. Whenever the line search procedure fails in the direction of the FMNR step, we reverse the search direction and usually find a minimum energy point in the opposite direction. Although this procedure highly stabilizes the FMNR algorithm, and, in fact, this was the very procedure that gave us the first set of saddle points, it is biased toward finding minima. Another, much more effective procedure is to reduce the FMNR step by an appropriate factor to prevent large atomic movements. This procedure works extremely well in the early stages, but unnecessarily slows down convergence toward the end of the minimization by further reducing the already small FMNR steps. A better solution is when an absolute limit is applied to the FMNR step, i.e., the full FMNR step is taken if it is shorter than the limit and it is reduced to the limit otherwise (a similar idea to the trust region concept). With this latter procedure we were able to find saddle points with a comparable rate to finding minima. Although there were a few cases when the FMNR minimization diverged or stalled in endless oscillation, the number of these unsuccessful minimizations was negligible compared to the large number of successful ones.

To find the pair of minima associated with a particular saddle point, i.e., identification of MSM triads, is straightforward. A small step away from a saddle point in the two opposite directions of negative canonical curvature on the potential energy hypersurface slightly lowers the energy, and subsequent energy minimization *usually* goes further downhill to the bottom of the two energy valleys sharing that particular saddle point. The two opposite directions of negative canonical curvature are defined by the eigenvector and its negative, respectively, associated with the single negative eigenvalue of the non-mass-weighted Hessian matrix at the saddle point. This means that a set of (low-energy) saddle points can be used to identify individual MSM triads which then can be used as building blocks to build the complete NCI (see the Computations section).

Two conformational search methods were used in conjunction with the TNCG/FMNR minimization procedure to locate saddle points on the potential energy hypersurface of the members of the C_4–C_{12} cycloalkane series: a systematic search method termed systematic unbounded multiple minimum search[16] (SUMM), and our new Monte Carlo search technique termed torsional flexing[17] (FLEX). SUMM when applied to cyclic structures proceeds by opening the ring, systematic variation of the remaining torsion angles of the temporarily acyclic molecules, and then reclosure of the ring. The resulting structures are subjected to energy minimization. The SUMM procedure operates on the variable torsion angles by randomly selecting values for torsion angle variation from a fixed set of torsion angles appropriate for a systematic search initially conducted at 120° resolution. When this set has been exhausted, torsion angles are selected from those appropriate for increasingly higher resolution. Torsional flexing is a local torsional rotation about a ring bond that preserves the atomic position of most of the ring atoms. FLEX can best be described by considering a torsion angle in the ring X–A–B–C–D–Y in which the ring bond between X and A, as well as the one between D and Y, is cleaved, resulting in two fragments. A (and its substituents) and all other connections to B (and their substituents) are rotated in one direction about the B–C bond, whereas D (and its substituents) and all other connections to C (and their substituents) are rotated in the opposite direction, about the B–C bond by a random angle. Reclosure of the ring generates a structure that is then subjected to energy minimization as described in the next section.

Computations

Conformational searches were conducted using a modified version of the MacroModel/BATCHMIN 3.1 computational chemistry program package[18a] running on a Silicon Graphics 4D/280 server. The selected force field was MM2 which has long been used successfully for conformational energy calculations of hydrocarbons.[19] The SUMM procedure is available within BATCHMIN 3.1,[18b] and our modified version allows for torsional flexing. The structures generated by the conformational

(15) Ponder, J. W.; Richards, F. M. *J. Comput. Chem.* **1987**, *8*, 1016–1024. Schlick, T.; Overton, M. *Ibid.* **1987**, *8*, 1025–1039.

(16) Goodman, J. M.; Still, W. C. *J. Comput. Chem.* **1991**, *12*, 1110–1117.

(17) Kolossváry, I.; Guida, W. C. *J. Comput. Chem.*, in press.

(18) (a) Mohamadi, F.; Richards, N. G. J.; Guida, W. C.; Liskamp, R.; Lipton, M.; Caufield, C.; Chang, G.; Hendrickson, T.; Still, W. C. *J. Comput. Chem.* **1990**, *11*, 440–467. MacroModel/BATCHMIN is available from Professor W. Clark Still, Columbia University, New York, NY 10027. (b) In BATCHMIN Version 3.1, the SUMM procedure is referred to as SPMC (for systematic pseudo-Monte Carlo search).

(19) Allinger, N. L. *J. Am. Chem. Soc.* **1977**, *99*, 8127–8134. A recent study has found that MM2 and ab initio calculations are consistent in the relative energies and geometries of conformers of the C_5–C_8 cycloalkane series. Ferguson, D. M.; Gould, I. R.; Glauser, W. A.; Schroeder, S.; Kollman, P. A. *J. Comput. Chem.* **1992**, *13*, 525–532. A new MM3 force field has been recently developed for hydrocarbons in Professor Allinger's laboratory: Allinger, N. L.; Yuh, Y. H.; Lii, J.-H. *J. Am. Chem. Soc.* **1989**, *111*, 8551–8566. Lii, J.-H.; Allinger, N. L. *Ibid.* **1989**, *111*, 8566–8575. Lii, J.-H.; Allinger, N. L. *Ibid.* **1989**, *111*, 8576–8582.

search procedures were first subjected to initial energy minimization using the TNCG algorithm available in BATCHMIN 3.1. The modified BATCHMIN was instructed to switch to FMNR minimization after the energy gradient dropped below rmsG = 30 kJ/mol·Å. The FMNR algorithm was then used to fully minimize the structures. Analytical first and second derivatives of the molecular mechanics potential energy were used for TNCG and FMNR minimizations, and the three translational and three rotational degrees of freedom were removed from the Hessian matrix using the Eckart constraints.[11b] The FMNR algorithm is available in BATCHMIN; however, certain modifications were required to achieve good convergence. The standard FMNR command in BATCHMIN can be instructed to use a factor <1 to reduce every FMNR step so that large atomic movements can be avoided. It was suggested, however, in the Theory section that faster convergence could be achieved by applying an absolute limit to the FMNR step size. The FMNR command has been modified accordingly, and an absolute limit of 5 Å was applied to the FMNR step size; i.e., the sum of all atomic movements was limited to 5 Å at each FMNR iteration. Another small modification has also been implemented. BATCHMIN does not allow the energy to increase during FMNR minimization. However, occasionally uphill movement is required to reach the nearest saddle point (or multiple maximum) on the potential energy hypersurface. Therefore, our modified BATCHMIN 3.1 allows energy increases of up to 5 kJ/mol during FMNR minimization. The quadratic line search routine in BATCHMIN has also been modified to allow for the reversal of the search direction, but this option was not used (see the Theory section). The fully minimized structures (rmsG < 0.01 kJ/mol·Å) were compared with those previously found based on superimposition of the ring atoms, and only unique structures were stored. Enantiomeric conformers were not distinguished and the comparison included symmetry operations to detect if two structures, which appeared to be different, were simply subject to a rotation and/or reflection of the numbering system of their ring atoms. The unique structures were also compared with respect to their energy, and only those within a specified energy window above the global minimum were saved. Our goal was to conduct a comprehensive conformational analysis; therefore, an extremely wide energy window of 150 kJ/mol was applied. The output files of fully minimized unique structures generated by SUMM and FLEX were compared and a combined file was generated. This procedure was found to be unnecessary for small molecules, but we have found that it is useful for larger molecules whose conformational space becomes increasingly complex. An exhaustive search cannot be assured by using SUMM[20] or FLEX. It can only be accomplished by a grid search procedure performed at high resolution which in turn requires enormous computational resources when applied to larger molecules. Nonetheless, identical or at least very similar results obtained independently by a systematic and a Monte Carlo conformational search technique imply that the vast majority of minima and/or saddle points has been found. This is especially true for the low-energy structures, because both SUMM and FLEX have been used with the so-called usage-directed search option that has been found to focus conformational searches very effectively toward low-energy regions of the potential energy hypersurface.[21]

The combined output file of the SUMM and FLEX searches contained minimum energy structures, transition-state (saddle point) structures, and a few multiple minimum structures. The output file was then subjected to a procedure termed XTST which is an extended version of the standard BATCHMIN normal mode analysis command termed MTST. XTST uses the non-mass-weighted Hessian matrix to find the transition-state structures. Furthermore, XTST generates two structures slightly distorted along the direction indicated by the eigenvector (and its negative) associated with the single negative eigenvalue of the Hessian matrix for each and every transition-state structure, as described earlier in the Theory section. The output file of the XTST procedure contained these structure triads (a transition-state structure and two other structures slightly lower in energy). These distorted structures were then subjected to energy minimization with the TNCG algorithm to fully minimize them. This procedure generated the file of the MSM triads. The minimum energy conformers in the MSM triads were comparable to the ones discovered during the SUMM and FLEX searches. It is noteworthy that the set of minimum energy conformers found during the SUMM/FLEX search occasionally contained additional conformers relative to the ones produced by the (indirect) XTST procedure (see Results and Discussion section).

(20) The SUMM procedure like other systematic search procedures could, in principle, perform an exhaustive search. However, although SUMM is more efficient than other systematic search techniques, SUMM usually cannot reach the resolution required for an exhaustive search with flexible molecules.

(21) Chang, G.; Guida, W. C.; Still, W. C. *J. Am. Chem. Soc.* **1989**, *111*, 4379–4386.

The file of the MSM triads served then as input for a companion program of BATCHMIN termed XNET. XNET uses the MSM triads to build the NCI by a simple procedure. The MSM triads are read sequentially, and the minima are checked for uniqueness with a procedure similar to the one used during the conformational searches. Two MSM triads share zero, one, or both minima. Sharing zero minima means there is no direct connection between the two MSM triads. Sharing one minimum means that two saddle points are connecting the same energy valley to two different energy valleys. Sharing both minima means there are two different saddle points connecting the same pair of energy valleys. The list of this pairwise connectivity information defines the NCI. There is, however, a special class of saddle points which has not yet been accounted for. There are saddle points which appear to reconnect a minimum to itself. In fact, these saddle points are of two different kinds; they either reconnect a minimum energy structure to an identical structure or connect two enantiomeric forms of the same minimum energy conformer (the comparison procedure used does not distinguish enantiomers). The former case occurs when a conformer simply interconverts to an identical form which is only subject to a rotation and/or reflection of the numbering system of the ring atoms. The latter case is of particular importance; indeed, the saddle points connecting enantiomers represent the "bridges" between two mirror image potential energy hypersurfaces. The transition states associated with these saddle points allow for the interconversion of nonsuperimposable "left-handed" and "right-handed" conformers of a molecule. XNET can be instructed to prune the NCI by specifying an energy window for the minima and another energy window for the saddle points. Furthermore, multiple saddle points connecting the same pair of energy valleys can be eliminated considering only the lowest energy saddle point. When XNET was used with a 25-kJ/mol energy window for the minima and a 50-kJ/mol energy window for the saddle points, multiple saddle points were eliminated.

XNET provides three different ways of visualizing the NCI and the different modes of interconversion. The (pruned) NCI can be plotted on a three-dimensional "staircase" diagram (see Figures 1–5). The steps on the staircase represent the minima. The height of the steps is proportional to the strain energy of the minimum energy conformers. The term strain energy is used to define the (MM2) *steric energy difference* between minimum energy conformers or transition states and the global minimum energy conformer. The connections between the steps represent the saddle points. The height of the connections is proportional to the strain energy of the transition-state structures. The connections are ordered according to increasing height from the front toward the back. The top of a connection is shifted from the middle to the right by an extent proportional to the reciprocal ratio of the steric energy difference between the saddle point and the higher energy minimum and the steric energy difference between the saddle point and the lower energy minimum. Two output options are provided by XNET to study the different modes of conformational interconversion. One option is a file of the individual MSM triad structures superimposed in different colors. We found this output file to be an extremely useful tool to study the modes of interconversion. Figures 6–20 are stereo plots of MSM triads showing the minimum energy conformers in bold. Particular modes of interconversion are highlighted by the use of color. The ring bonds participating in a particular mode are colored in the following way: red and blue in the two minimum energy structures, respectively, and green in the transition-state structure. The other output option is a "movie" file which is a series of up to a few thousand (...–minimum–saddle–minimum–saddle–...) structures whose sequence is determined by a quasi-Metropolis Monte Carlo[22] simulation at a high temperature (600 K) to allow for high-energy interconversions. The simulation is run on the complete NCI, and only those steps between neighboring local minima connected by a saddle point are allowed. This means that the Monte Carlo simulation is constrained in that it is restricted to the routes in conformational space defined by the NCI. The Metropolis criterion, based on the MM2 steric energy difference between neighboring minima, is applied to determine the sequence of minimum energy conformers, i.e., which conformers correspond to the frames 1, 3, 5, etc., in the movie. Moreover, the interconnecting transition states (frames 2, 4, 6, etc.) are also selected by using the Metropolis criterion based, however, on the steric energy difference between the saddle point and the current minimum. This means that lower energy transition states between the same two minimum energy conformers are favored over higher energy ones (if there is more than one transition state) by the Boltzmann factor. Note that this simulation has no thermodynamic value (e.g., it does not reproduce the Boltzmann distribution of the minimum energy conformers); nonetheless, lower energy conformers are visited more frequently, and animation by

(22) Metropolis, N.; Rosenbluth, A. W.; Rosenbluth, M. N.; Teller, A. H.; Teller, E. *J. Chem. Phys.* **1953**, *21*, 1087–1092.

Table I. Number of Local Minima and Saddle Points Found for the C_4–C_{12} Cycloalkane Series on the MM2 Potential Energy Hypersurface within a 150-kJ/mol Energy Window above the Global Minimum

	no. of minima[a]	no. of saddles[b]
C_4	1	1
C_5	1	1
C_6	2	2
C_7	2	2
C_8	4	9 (7)
C_9	8 (6)	17 (7)
C_{10}	18 (14)	50 (24)
C_{11}	38 (17)	142 (37)
C_{12}	117 (21)	462 (36)

[a] The numbers in parentheses correspond to a 25-kJ/mol energy window. [b] The numbers in parentheses correspond to a 50-kJ/mol energy window with only the lowest energy saddle point being considered between two particular minima.

the MacroModel movie option provides vivid insight to the internal motion of the ring atoms during continuous conformational interconversion.

Results and Discussion

The number of unique minima and saddle points found on the MM2 potential energy hypersurface of the C_4–C_{12} cycloalkane series is shown in Table I. The total number of minima and saddle points within the 150-kJ/mol energy window clearly illustrates the rapidly increasing complexity of conformational space with increasing ring size. Although we cannot be absolutely sure that a truly comprehensive conformational search has been carried out, the results described below imply that, with the exception of cyclododecane, there can only be very few if any undiscovered saddle points within the 150-kJ/mol energy window. It is instructive to note that the theoretical total number of saddle points is unknown. All that can be said is that the results in Table I do not violate the so-called Morse inequalities.[7c] As far as the theoretical minimum number of saddle points is concerned, one would expect that there is at least one saddle point (possibly very high in energy) associated with each and every pair of minima. In other words, a sufficiently wide energy window would afford at least $M(M-1)/2$ saddle points where M is the number of minima. However, this is not likely to be the case with potential energy hypersurfaces (especially those of ring molecules) where certain conformational interconversions would require passing *infinite* energy barriers by, e.g., breaking a bond. This means that, because of the discontinuous nature of potential energy hypersurfaces, the number of saddle points is expected to be far less than the number necessary to connect each and every pair of minima.

The FLEX and SUMM searches gave identical results for all rings up to and including cyclodecane, and every unique saddle point was found at least 10 times. Both FLEX and SUMM found 137 unique saddle points for cycloundecane. Among them a few high-energy saddle points were only found once, which implies that neither FLEX nor SUMM alone could find all the saddle points. Nonetheless, the combined result of the FLEX and SUMM searches afforded only a few more (142) saddle points and thus was indicative of a comprehensive search, because the combined search found each of the 142 saddle points at least twice, and the majority of the saddle points were found more than five times. Cyclododecane, however, has proven to be too difficult for even a very extensive combined SUMM/FLEX search which took over one CPU week each. FLEX found 328 saddle points and SUMM found 429 saddle points. We believe that the combined result of 462 saddle points, although many of them were found only once, represents a reasonably complete search (especially in the lower region of the energy window). Saunders has recently presented a very extensive conformational study of the C_9–C_{12} cycloalkanes, in which a search for all minimum energy conformers was described.[10] In this study 8 minima for cyclononane, 18 for cyclodecane, 40 for cycloundecane, and 111 for cyclododecane were found. Our XTST procedure found the same

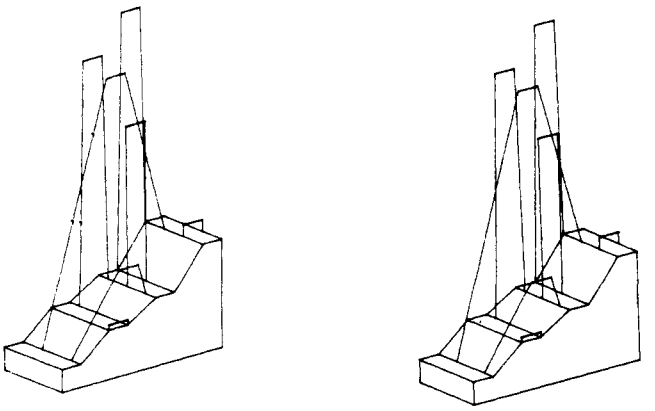

Figure 1. Staircase diagram of the cyclooctane NCI.

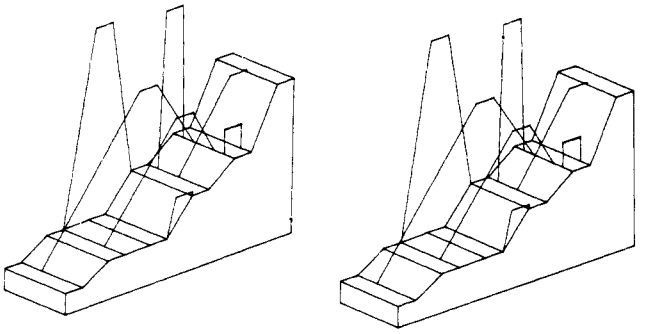

Figure 2. Staircase diagram of the cyclononane NCI.

number of minima for cyclononane and cyclodecane, but only 38 for cycloundecane. The two missing minima are #37 and #40 in Saunders' study. Although both of them are within the 150-kJ/mol energy window (88.2 and 142.2, respectively), we believe that our search did not locate them, simply because these high-energy minima are not associated with saddle points within the 150-kJ/mol energy window. *Note that our search procedure derives the minima indirectly from the saddle points.* As a matter of fact, the initial SUMM/FLEX search did find all of the 40 known cycloundecane conformers. As for cyclododecane, the SUMM/FLEX search found 121 conformers (10 more than Saunders). Four fewer (117) cyclododecane conformers were generated indirectly from the saddle points by the XTST/XNET procedure.

It should be noted that our goal was to conduct a comprehensive conformational search using a wide energy window. This study was intended to show that such a comprehensive (or reasonably comprehensive) analysis was indeed possible using contemporary hardware and software resources. With larger molecules than cyclododecane, however, this kind of analysis could push readily available computational resources beyond their limit. Nonetheless, such an analysis is usually not necessary. Conducting the conformational searches within a thermodynamically reasonable, much smaller energy window, is much less computationally intensive, especially when a usage-directed search[21] is applied. Table I also shows the number of minima and saddle points of the C_4–C_{12} cycloalkane series found within a thermodynamically reasonable energy window (25 kJ/mol for the minima and 50 kJ/mol for the saddle points). The number of saddle points was further lowered by focusing on the kinetically most probable conformational interconversions, i.e., considering only the lowest energy saddle point between the same two minima. These restrictions define a largely pruned NCI whose determination is, in our view, the goal of a rigorous conformational analysis. Note that direct use of a 50-kJ/mol energy window in the conformational searches can produce the same NCI for cyclododecane in hours as opposed to weeks using a 150-kJ/mol energy window (and subsequent pruning). This very fact implies that our approach to conformational analysis can readily be employed for molecules more flexible than cyclododecane.

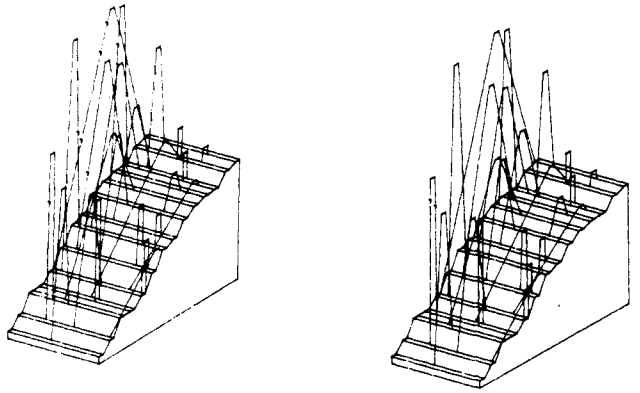

Figure 3. Staircase diagram of the cyclodecane NCI.

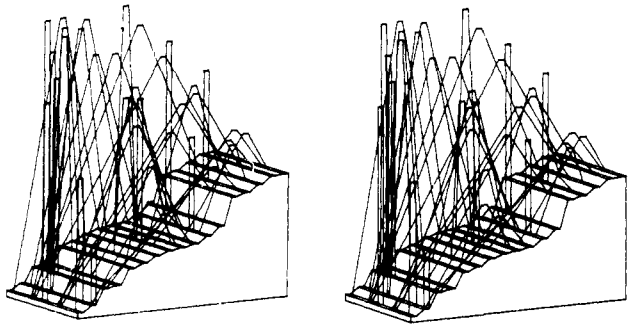

Figure 4. Staircase diagram of the cycloundecane NCI.

Staircase diagrams of the NCI's determined for cyclooctane to cyclododecane are shown in stereoplots in Figures 1–5. The NCI's were pruned to be realistic thermodynamically (25-kJ/mol energy window for the minima and 50 kJ/mol for the saddle points representing the lowest barrier between two minima). Table II contains detailed information about the individual MSM triads for the whole C_4–C_{12} cycloalkane series. The MSM triads are ordered (and numbered) according to increasing steric energy of the transition state. Each MSM triad is represented by two lines. Interconversions between identical forms of the same conformer (only subject to a rotation and/or reflection of the numbering system of the ring atoms) and MSM triads representing the "bridges" between mirror hypersurfaces (associated with the "left-handed" and "right-handed" forms, respectively) are marked by an open circle and an asterisk at the beginning of the first line, respectively. This line contains the strain energy of the lower energy minimum (MM2 steric energy relative to the global minimum), the steric energy difference between the two minima, and the steric energy difference between the saddle point and the lower energy minimum. Two additional fields in the first line describe the mode of interconversion exhibited by that particular MSM triad. The first field is the code of the interconversion that is described below. Note that, with the exception of only four cases (marked by "?"), each particular mode of interconversion can be assigned unambiguously. There are, however, a number of interconversions (especially cycloundecane and cyclododecane interconversions) which exhibit the different modes less clearly, with a certain degree of "noise" involved. The second field identifies well-known interconversions (e.g., chair to twist boat (C-TB) in cyclohexane). The second line associated with a particular MSM triad displays the torsion angle *differences* between the two minima. The torsion angle differences were found to be very useful in identifying the different modes of interconversion.

Cyclobutane. Cyclobutane has one single nonplanar minimum energy conformer which can be constructed by fusing two triangles at an angle of ca. 145°.[1c] Interconversion between two identical forms of the cyclobutane conformer requires 4.0 kJ/mol of energy via a planar transition-state geometry which spans a square (see Table II).

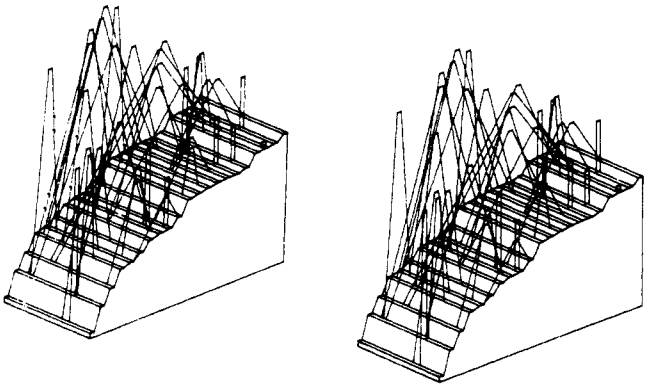

Figure 5. Staircase diagram of the cyclododecane NCI.

Cyclopentane. Cyclopentane has been described in terms of 10 envelope and 10 twist conformations interconverting via free pseudorotation.[1d,2] This picture, however, is highly redundant from the perspective of ring symmetry. Rotation and/or reflection of the numbering system of the cyclopentane ring atoms reduces the number of minimum energy conformers to one single enantiomeric pair of twist conformers "bridged" by the envelope conformation. On the MM2 potential energy hypersurface the true envelope conformation with four coplanar ring atoms corresponds to the saddle point connecting the enantiomeric pair of the slightly twisted minimum energy conformers. Nonetheless, the energy required to cross the "mirror-bridge" is essentially equal to zero.

Cyclohexane. Stereoviews of the well-known twist-boat to twist-boat (TB–TB) and chair to twist-boat (C–TB) interconversions are shown in Figures 6 and Figure 7, respectively. The twist-boat conformer interconverts to its enantiomer (via pseudorotation[4c]) through the boat conformation which is a saddle point on the MM2 potential energy hypersurface. The boat conformation exhibits a very-low- (4.6 kJ/mol) energy barrier. The C-TB interconversion (symmetrical mode[4c]) crosses a fairly-high-energy barrier (44 kJ/mol) through an asymmetrical, slightly twisted form of the symmetrical, so-called half-chair conformation. It is instructive to note that, although the two interconversions seem to be of a different nature, in fact, Figures 6 and 7 clearly show that both exhibit the very same kind of coordinated atomic movement. We have termed this atomic movement kayaking, because it involves three ring bonds A–B–C–D following a moving pattern very similar to the pattern exhibited by the coordinated movement of the kayaker's arms and the double-bladed paddle. Kayaking is associated with characteristic torsion angle differences between the two minima (see Table II). There is a significant change in the middle torsion angle (B–C) and a smaller change in both the other torsion angles (A–B and C–D) that is opposite to the change in the central torsion angle. This torsion angle difference pattern is denoted by "+/−−/+" (or "−/++/−"). The TB–TB interconversion exhibits two kayaking patterns, both associated with the −33°/62°/−33° torsion angle difference triplet (underlined in Table II). The C–TB interconversion exhibits one kayak pattern associated with a 87°/−120°/87° triplet (underlined in Table II). The B–C torsion angle is nearly eclipsed in the transition state. It has been found that kayaking is not an isolated case in cyclohexane; indeed, kayaking is one of two basic modes identified in the conformational interconversions exhibited throughout the C_6–C_{12} cycloalkane series.[23] Note, however, that kayaking has different, although less frequently encountered versions which will be introduced later. This particular version of kayaking is coded "K3" in Table II.

Cycloheptane. The cycloheptane NCI is similar to the cyclohexane NCI, but there are significant differences. Unlike cyclohexane, cycloheptane interconverts between the two mirror hypersurfaces within the chair family, rather than the boat family. The minimum energy conformer is the twist-chair form (and its

(23) Prior to initiating this investigation, we had noted kayaking as a potential mode of conformational interconversion while examining Dreiding models of medium ring cycloalkanes.

Table II. Modes of Conformational Interconversion in the C_4–C_{12} Cycloalkanes[a]

cyclobutane

o 1 0.0 0.0 4.0
-40 40 -40 40

cyclopentane

* 1 0.0 0.0 0.0
17 -13 21 8 -9

cyclohexane

* 1 22.4 0.0 4.6 K3K3 TB-|B|-TB see Figure 6
62 -33 -33 62 -33 -33
2 0.0 22.4 44.0 K3 C-TB see Figure 7
87 -25 -8 -25 87 -120

cycloheptane

* 1 0.0 0.0 4.2 K3F22 TC-|C|-TC see Figure 8
-49 78 -49 -15 18 18 -15
2 0.0 13.2 30.2 K3 TC-TB
-6 -6 -23 89 -127 89 -23

cyclooctane

* 1 4.0 0.0 0.8 F22F22 TCC-(CC|-TCC see Figure 9
-22 26 26 -22 -22 26 26 -22
2 0.0 7.0 11.7 K3 BC-|TBC|-TBC see Figure 10
-18 5 10 22 -24 -53 91 -53
o 3 13.1 0.0 1.8 F22F22 TB-|BB|-TB
29 -29 -29 29 29 -29 -29 29
* 4 7.0 0.0 24.4 K3-K3- TBC-|C|-TBC
-28 -45 98 -45 -28 -45 98 -45
5 0.0 13.1 38.4 K3 BC-TB
0 -7 37 -104 133 -65 -21 28
6 4.0 2.9 37.0 ? TCC-TBC
-7 -63 132 180 132 -63 -7 26
7 7.0 6.1 38.8 7 TBC-TB
-129 -16 84 -52 11 -16 -56 154

cyclononene

1 3.2 6.1 6.8 F22F22- TCC-TCTC see Figure 11
21 29 -32 -33 30 17 -30 -5 -18
* 2 13.2 0.0 4.3 K3 SCB-SCB
5 2 -12 -12 2 5 52 -75 52
3 3.1 10.1 18.3 K3 TCB-SCB
16 63 -103 65 18 -26 2 -13 -3
4 9.3 14.4 14.8 F22F22- TCTC-SCC
-26 -40 29 20 -33 -27 25 7 20
5 0.0 13.2 25.8 K3 TBC-SCB see Figure 12
73 22 -19 -5 -8 -5 13 68 -109
6 9.3 3.9 27.5 K3 TCTC-SCB
64 26 -7 -10 -8 14 -39 125 -146
7 3.1 6.2 33.7 K3 TCB-TCTC
-4 -11 -81 157 -126 38 -15 17 6

cyclodecene

* 1 6.4 0.0 5.4 F3F22F3 BCC-|BCC|-BCC see Figure 13
9 -14 -45 23 23 -45 -14 9 14 14
2 1.8 10.7 10.9 F2-F2F22-
-32 -13 30 4 15 -20 -10 -19 23 42
* 3 9.5 0.0 5.3 F22-F22-
-32 -2 -26 31 31 -26 -2 -32 21 21
4 12.5 0.8 5.1 F2-F2F22-
-29 -45 26 27 -15 -15 -19 10 8 34
5 6.4 11.4 12.6 F2-F2F22-
28 4 15 -10 -13 -34 34 42 -29 -18
6 9.5 3.0 10.5 K3
2 -9 -62 91 -69 -14 7 12 -1 7
7 15.7 1.9 5.8 F22-F22-
10 30 -24 -28 18 10 30 -24 -28 18
8 19.9 0.7 2.4 K3
65 -45 2 -4 9 -6 9 -4 2 -45
* 9 17.8 0.0 5.0 F3F22F3
-19 -1 20 20 -1 -19 -29 36 36 -29
o 10 4.8 0.0 18.4 k5k5 TCCC-|TCCC|-TCCC see Figure 14
62 0 -62 16 16 -62 0 62 -16 -16
11 1.8 4.6 22.7 K3 TBCC-BCC
-14 3 5 7 8 12 -16 -78 110 -72
12 4.8 15.1 20.3 7
28 15 -3 -62 -5 57 -5 -62 -3 15
* 13 19.9 0.0 5.4 F3F22F3
-10 24 6 6 24 -10 -43 49 49 -43
14 0.0 4.7 26.7 K3 BCB-|BTCB|-TBC
-73 -13 -2 13 6 11 -3 -13 -74 116
15 9.5 6.2 20.0 K3
80 28 -17 -5 1 -1 -20 21 71 -120
16 4.7 12.4 25.0 K3
4 4 5 12 7 -13 -72 108 -73 -12
17 13.3 4.5 18.3 K3
81 10 12 -14 -8 4 -18 23 74 -122
18 1.8 2.9 30.0 K3
35 -13 11 5 8 -4 -12 -83 165 -130
19 17.8 2.8 21.0 K3
9 -20 31 81 -122 62 11 18 -7 -11
20 12.5 5.3 26.9 K3
12 6 4 -15 -82 113 -64 -28 11 6
21 9.5 8.2 31.2 K3
-17 28 84 -128 76 21 -20 3 -7 0
22 6.4 6.1 41.3 K3
-88 -32 21 -1 3 14 -6 -10 -78 134

Table II (Continued)

23 17.8 0.8 31.0 K3
-14 8 56 -144 156 -73 -25 16 11 3

24 6.4 14.2 41.7 F22
11 -10 7 46 -112 94 64 -55 -34 18

cycloundecane

o 1 1.1 0.0 11.0 F3k5F3
-36 -4 4 36 -6 7 -64 0 64 -7 6

2 3.9 6.4 12.4 k5k5-
42 -14 -68 22 22 -58 -7 23 10 -5 4

3 1.1 8.8 17.6 K3
26 2 -2 -15 -10 -10 9 30 50 -101 69

4 3.9 14.9 19.7 F2-F2F22-
-10 -1 2 -50 33 46 -68 -49 29 11 30

5 0.0 1.1 23.9 K5F3F3
7 97 -131 110 2 -47 33 8 15 -28 -8

6 7.1 2.8 17.5 K3
-16 14 6 21 -1 -5 -3 -6 -64 104 -91

7 11.5 8.5 15.3 k5k5-
55 7 -54 -9 14 26 20 1 -59 5 -14

8 7.8 13.5 19.8 K3-F22-
20 -21 55 -94 46 12 22 13 -29 -38 23

9 10.3 11.2 18.1 F2K3-
-17 -35 36 75 -107 59 2 0 2 0 4

* 10 11.5 0.0 17.1 k5K3k5 see Figure 17
-81 106 -51 -56 -5 10 20 20 10 -5 -56

11 9.6 11.9 19.4 F22F3F2-
50 62 -78 -48 25 10 31 -22 -6 -11 -27

12 0.0 18.2 29.6 K3
20 12 64 -138 61 45 6 -47 -15 0 14

13 0.0 11.5 31.3 K3
-14 -7 0 -2 -11 -3 13 86 -121 73 26

14 0.0 20.0 34.3 K3-k3
-116 28 13 16 16 12 -9 -60 -7 80 60

15 1.1 10.4 34.0 K3
-14 0 -10 -20 2 4 16 80 -119 91 10

16 4.3 17.0 31.4 F22-F2-
46 36 -19 -35 -99 126 -45 -19 14 -6 -24

o 17 9.6 0.0 26.1 F22F3F22
-79 -56 68 61 0 -61 -68 56 79 -15 15

18 7.8 1.7 28.1 F22
21 20 -35 15 14 -53 -20 -21 121 -86 -64

* 19 0.0 0.0 36.3 F3F3K5 see Figure 15
114 -97 1 5 38 -14 -14 38 5 1 -97

20 9.9 10.1 26.6 k5K3k5
-21 -1 -33 -5 11 19 88 -124 53 50 3

21 7.1 4.4 30.1 F3F3K5
0 -2 95 -122 103 9 -41 14 14 17 -37

* 22 18.7 0.0 20.0 K3-F22-
-4 17 27 -45 -45 27 17 -4 59 -105 59

23 1.1 6.0 38.4 K3
-21 12 2 0 9 0 21 -19 -92 127 -84

24 1.1 2.8 38.8 k3
34 29 -34 -9 21 10 10 20 -143 -35 136

25 0.0 21.3 41.6 F2
0 -4 -32 -15 -2 61 9 -76 -86 128 -33

26 0.0 13.0 43.0 K3
-49 -3 12 -10 -8 -4 2 8 84 -173 150

27 0.0 10.3 43.0 k3
15 10 35 -71 -6 99 26 118 -169 -25 -44

* 28 13.0 0.0 30.9 ?
144 -75 -7 -6 -6 -7 -75 144 0 -153 0

o 29 3.9 0.0 40.2 k5F2FkF2
0 -75 2 61 21 111 -111 -21 -61 -2 75

30 3.9 3.2 42.6 k3
-24 -23 14 4 19 -30 -28 -148 31 146 -12

31 1.1 18.9 45.9 K3
89 -4 19 -9 -27 -1 6 -13 33 86 -134

32 3.9 5.7 43.5 FkF2-k5-
50 -21 -36 -122 113 11 38 50 -10 -79 2

33 3.9 3.9 43.8 k3F22F22
0 157 36 -177 11 -19 -84 26 93 -55 -70

34 1.1 9.2 47.5 k3
-156 11 8 24 -3 -2 0 16 17 175 -21

35 3.9 0.4 45.1 K3
-155 161 -82 -6 7 6 2 5 -10 8 56

36 0.0 9.6 49.1 k3 see Figure 16
-9 9 -24 150 40 -166 -19 -19 7 -2 -11

37 9.9 1.6 40.0 K3
-32 -5 -8 6 -3 3 5 74 -127 94 40

cyclododecane

1 10.9 5.3 10.2 F3F3F2-
-41 1 -6 50 -7 -77 29 34 14 20 -4 0

o 2 23.1 0.0 1.0 F3F3F3F3 see Figure 18
-6 33 -10 -10 33 -6 6 -33 10 10 -33 6

* 3 14.6 0.0 9.5 k5k5
-16 9 9 -16 -26 1 72 -24 -24 72 1 -26

4 7.3 7.1 18.1 k5-F3
-13 88 1 -66 7 -10 15 -6 -23 3 63 -27

5 18.9 0.8 8.5 F2F3-
-21 70 15 -55 13 14 27 3 -3 -7 -16 -41

6 10.9 3.5 16.5 k3
-2 3 -5 7 -13 8 -10 -88 -13 91 26 -21

o 7 20.7 0.0 6.7 F2 see Figure 20
49 25 10 -3 7 3 -3 -7 3 -10 -25 -49

8 14.6 5.5 13.6 k3
-13 -7 -81 -2 80 10 -4 15 -10 -5 5 26

9 14.4 0.3 14.6 K3
11 7 -4 -5 -7 -9 4 21 69 -102 53 8

o 10 20.2 0.0 9.3 k3-F2-F2-
-76 -12 -17 21 34 0 -34 -21 17 12 76 0

11 0.0 4.5 29.9 K3 [3333]-[2334]
15 88 -124 98 9 -13 -9 0 -2 -7 -5 -2

Table II (Continued)

12	4.5	5.9	26.7	K5	[2334]-[2343]							
	-1	110	-106	100	-11	-16	-9	12	6	0	-23	-15
13	4.5	7.5	27.0	K3k5F3-								
	-2	1	-71	112	-110	-15	8	24	15	3	-6	-8
14	0.0	10.9	31.8	k3								
	0	3	2	25	3	127	-16	-122	25	-5	4	2
* 15	23.3	0.0	10.2	k5k5-					see Figure 19			
	-5	7	7	-5	-41	2	61	-18	-18	61	2	-41
16	7.3	8.9	26.4	k5-k5-								
	2	72	2	-85	-10	19	11	23	11	19	-10	-85
17	19.7	4.8	14.5	K3								
	10	90	-108	50	1	14	11	-2	-2	-17	-18	11
18	19.7	3.6	14.7	F22F3								
	-5	17	20	11	-29	-79	55	64	-33	-19	10	-6
19	13.8	9.3	21.4	F22								
	81	43	-24	-14	4	-8	-2	29	8	30	-76	-71
20	13.8	6.4	22.3	K3								
	87	30	-13	-16	10	-3	-3	2	16	7	51	-107
21	20.2	0.0	17.3	K3								
	-14	34	17	-10	19	-11	9	-45	15	106	-95	36
22	20.2	2.7	18.1	k5-K3-								
	-23	-1	-32	8	44	11	-6	-17	-81	115	-47	4
23	20.2	2.9	18.1	F22								
	88	94	-131	73	34	-21	-19	38	5	27	-74	-55
24	14.6	5.6	24.0	F2K3-F3								
	25	25	-11	43	-100	100	9	-11	6	-41	-17	16
25	7.3	15.8	31.4	k5k3-								
	-25	-16	-17	-26	7	70	-7	-66	-14	-114	26	151
26	10.3	4.0	28.5	k3								
	-58	-7	29	13	-4	-2	-34	-14	-126	17	137	-13
27	7.3	16.0	33.3	K3								
	3	-17	-84	118	-80	-8	13	-4	3	-1	7	15
28	14.6	8.4	26.9	k5Fk-								
	0	-24	-38	-1	73	-7	-70	-19	-105	119	25	63
29	14.4	5.8	28.3	K3								
	27	-7	-6	-7	-1	4	-4	-76	144	-105	-56	28
30	4.5	15.7	39.3	k3								
	-2	9	-25	118	13	-125	-7	-10	10	1	-21	-9
31	4.5	6.4	39.4	F3FkF3-								
	17	10	-72	2	-127	112	6	53	10	4	-24	11
32	4.5	14.8	40.9	K3								
	3	7	74	-125	104	23	-8	-17	-14	-2	-1	9
33	10.9	8.0	36.8	K3								
	16	-30	-88	143	-85	-16	0	6	0	1	1	6
34	10.3	9.7	38.3	F2FkF2-								
	13	18	3	-3	-18	-13	-42	1	-113	113	-1	42
35	16.2	3.5	33.1	K3								
	13	-7	7	2	-8	6	-19	-72	129	-96	-25	8
36	10.9	9.3	39.0	K3								
	4	11	6	-30	-94	136	-72	-19	4	2	3	1

[a] Each MSM triad is represented by two lines. Interconversions between identical forms of the same conformer (only subject to a rotation and/or reflection of the numbering system of the ring atoms) and MSM triads, representing the "bridges" between mirror image hypersurfaces, are marked by an open circle and an asterisk at the beginning of the first line, respectively. This line contains the strain energy of the lower energy minimum (MM2 steric energy relative to the global minimum), the steric energy difference between the two minima, and the steric energy difference between the saddle point and the lower energy minimum. The mode of interconversion is described by a code string. "K3", "k3", "K5", and "k5" denote the four different kayaking modes. "F2", "F22", and "F3" denote single and double corner flapping, and handle flapping, respectively. "Fk" denotes a transition mode between flapping and kayaking. Hyphens in the code string represent "spacings" between the ring bonds involved in a particular mode. A "spacing" consists of one or more consecutive ring bonds that have not been significantly distorted during interconversion. The eight different modes are explained in the Results and Discussion section. The last field in the first line identifies well-known interconversions, e.g., pseudorotation of twist-boat enantiomers through the boat form in cyclohexane (TB–(B)–TB). The abbreviations are as follows: B, boat; C, chair; T, twist; and S, skewed.[25] The Dale nomenclature[28] is used for cyclododecane conformers. The second line associated with a particular MSM triad displays the torsion angle *differences* between the two minima. The difference patterns corresponding to the different modes of interconversion are underlined. A few torsion angle differences are printed in bold indicating an overlap between two different modes.

Figure 6. TB–TB interconversion in cyclohexane (#1), K3-kayaking mode shown in color.

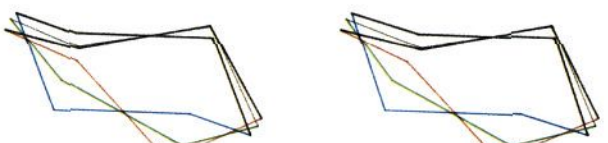

Figure 7. C–TB interconversion in cyclohexane (#2), K3-kayaking mode shown in color.

enantiomer) interconverting through the true chair transition-state form which exhibits a 4.2-kJ/mol energy barrier. The higher energy cycloheptane twist-boat conformer is less strained compared to the twist-chair conformer (13.2 kJ/mol) than the twist-boat form compared to the chair form in cyclohexane (22.4 kJ/mol). Similarly, the energy barrier between the two minimum energy conformers is less in cycloheptane (30.2 kJ/mol) than in cyclohexane (44 kJ/mol). The cycloheptane boat conformation, which is considered to be the transition state between pseudorotating

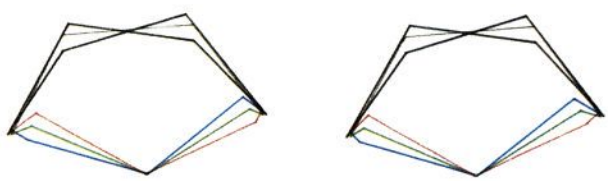

Figure 8. TC–TC interconversion in cycloheptane (#1), double corner flapping mode shown in color.

twist-boat forms,[1e] is not, in fact, a saddle point on the MM2 potential energy hypersurface. The TC–TB interconversion exhibits the same K3-kayaking mode (through an asymmetrical transition state) already seen in cyclohexane. The "mirror-bridge" interconversion between enantiomeric twist-chair conformers exhibits an interesting combination of two different modes, namely, the same K3-kayaking, and an entirely different mode termed double corner flapping ("F22"). Figure 8 shows the mode of double corner flapping which is the most frequently encountered version of the other basic mode of interconversion found throughout the C_6–C_{12} cycloalkane series. This mode is termed flapping in general, and it means that one or more ring atoms are flapped about a hinge comprised of two other ring atoms. Double corner flapping is a very-well-coordinated pattern of atomic movement where two adjacent corners (consecutive ring atom triplets) are flapped to opposite directions. One corner is flapped

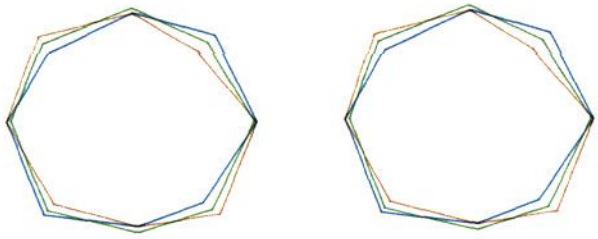

Figure 9. TCC–TCC interconversion in cyclooctane (#1), two double corner flapping modes shown in color.

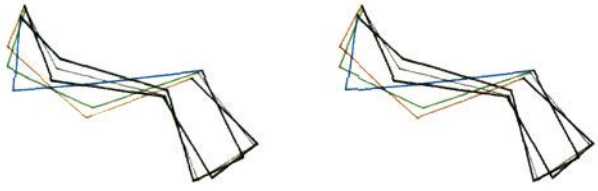

Figure 10. BC–TBC interconversion in cyclooctane (#2), K3-kayaking mode shown in color.

inward and the other corner is flapped outward. The torsion angle difference pattern associated with double corner flapping is a quadruplet of similar angles with alternating signs ("+/−/+/−" or "−/+/−/+"). It should be noted that (single) corner flapping has been suggested by Ōsawa as a universal mode of conformational interconversion in cycloalkanes and used successfully in conformational searches.[24] Ōsawa's corner flapping procedure, however, requires that the corner be flapped all the way to the opposite side of the average plane of the ring. We found only one single case of Ōsawa-type corner flapping (see below under cyclododecane). What we have found is that double corner flapping and all the other multiple flapping combinations which will be introduced later share a common pattern. Namely, there is always an alternating inward–outward flapping motion throughout the ring.

Cyclooctane. The cyclooctane conformers and their interconversion have been discussed in detail by Hendrickson[4] and Anet.[5a] The conformers have been classified into three families (boat–chair, chair–chair or crown, and boat–boat). Conformational interconversion within each family has been described via pseudorotation and ring inversion.[1f] Interfamily interconversion, BC–CC, in particular, has also been described. The MM2 potential energy hypersurface gives rise to four unique minimum energy conformers (see Figure 1). The BC family is represented by two conformers; one is the BC conformer itself (global minimum) and the other so-called TBC conformer which is 7 kJ/mol higher in energy. The CC family exhibits one single unique minimum, the so-called TCC conformer, which is only slightly more strained (4 kJ/mol) than the BC conformer. The single unique conformer of the BB family is the relatively high-energy TB conformer. TCC and TBC interconvert to their enantiomers through symmetric transition states (TCC through CC, and TBC through C). Identical TB conformers (subject to a reflection and rotation of the numbering system of the ring atoms) are connected via the BB transition state (see Table II). Figure 9 is a stereoview of the TCC–TCC interconversion displaying two double corner flapping modes which also occurs in the TB–TB interconversion. Note the alternating inward–outward flaps. The TBC–TBC interconversion consists of two disjoint K3-kayaking modes. Note that hyphens in, e.g., the "K3–K3–" code represent "spacings" between the ring bonds involved in a particular mode. A "spacing" consists of one or more consecutive ring bonds that have not been significantly distorted during interconversion (i.e., small torsion angle differences *not* underlined in Table II). The BC conformer interconverts within the BC family to TBC through another TBC form. The transition-state TBC is very similar to the minimum energy TBC. The only difference is that, unlike the minimum

(24) Gotō, H.; Ōsawa, E. *J. Am. Chem. Soc.* **1989**, *111*, 8950–8951.

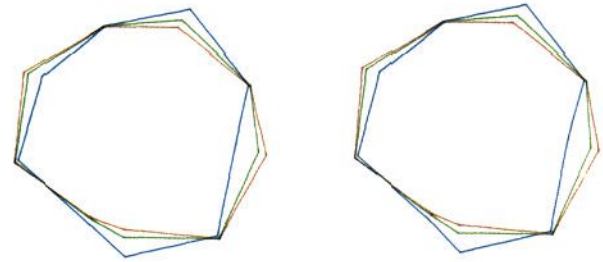

Figure 11. TCC–TCTC interconversion in cyclononane (#1), two double corner flapping modes shown in color.

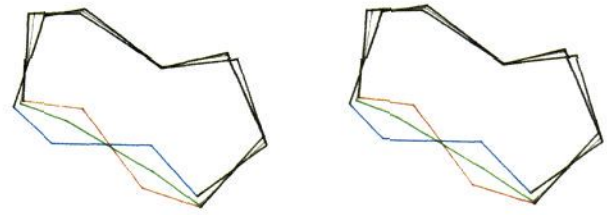

Figure 12. TBC–SCB interconversion in cyclononane (#5), K3-kayaking mode shown in color.

TBC, the saddle TBC has an unfavorable (near-zero) torsion angle which costs 4.7 kJ/mol in strain energy. The zero torsion angle is a consequence of the familiar K3-kayaking mode shown in Figure 10. The interfamily interconversions exhibit asymmetrical high-energy transition states. In fact, the TCC–TBC and TBC–TB interconversions do not seem to exhibit coordinated atomic movement at all, although the TCC–TBC interconversion is associated with a symmetrical pattern of torsion angle differences between the TCC and TBC forms (see Table II).

Cyclononane. Cyclononane has six minimum energy conformers within a 25-kJ/mol energy window. The global minimum is the highly symmetrical TBC form which (due to entropic effects), however, is significantly less populated than that calculated from the Boltzmann distribution based on steric energy alone.[10] The other five conformers are TCB, TCC, TCTC, SCB, and SCC.[25] It should be noted that Anet has called the TCTC and SCC conformers into question.[9] Indeed, SCC collapses into TCTC and TCTC, then further collapses into TCC, crossing extremely low barriers (0.4 kJ/mol and 0.7 kJ/mol, respectively). There is no doubt that TCTC and SCC seem to have little, if any, thermodynamic significance. SCC is a high-energy terminal node on the cyclononane NCI, and we need not consider it further. TCTC, however, presents a different story. If the TCTC form exists for at least one vibration of the corresponding normal modes, then TCTC can be considered as a special low-energy transition structure that connects more than two minimum energy conformers. In other words, although TCTC does not seem to have thermodynamic significance, kinetically, TCTC seems to be an important intersection on the cyclononane NCI. The collapse of TCTC into TCC via two simultaneous double corner flapping modes is shown in Figure 11. Conformational interconversions in cyclononane have been studied qualitatively by Hendrickson[4c] and by Dale.[5b] The results of our quantitative analysis are shown in Figure 2 and Table II. Cyclononane exhibits particularly-low-energy barriers between minimum energy conformers in accordance with cyclononane's well-known high flexibility. Interestingly, the global minimum TBC form has only one connection to the relatively high-energy SCB form. The mode of this interconversion is the familiar K3-kayaking shown in Figure 12. Cyclononane exhibits only one "mirror-bridge" (within the 50-kJ/mol energy window) between the SCB enantiomers. The energy required to cross the "mirror-bridge" is 4.3 kJ/mol via K3-kayaking. The TCB and TCC forms are very close to each other in energy, but there is no *direct* connection between them.

(25) Ferguson, D. M.; Glauser, W. A.; Raber, D. J. *J. Comput. Chem.* **1989**, *10*, 903–910.

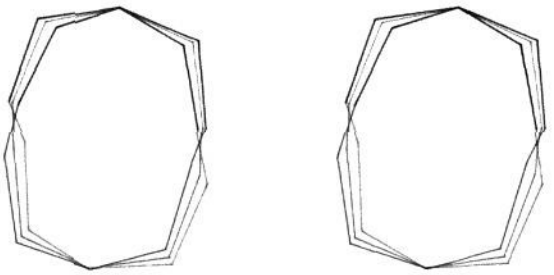

Figure 13. BCC–BCC interconversion in cyclodecane (#1), two handle flapping modes shown in color.

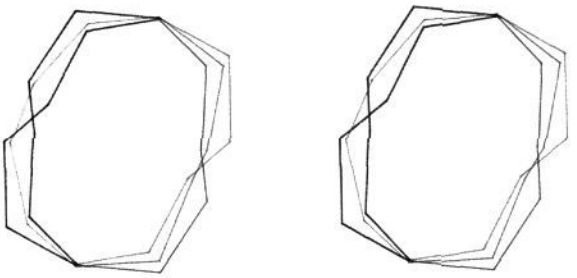

Figure 14. TCCC–TCCC interconversion in cyclodecane (#10), k5-kayaking mode shown in color.

Nonetheless, the TCTC form can be considered as a special transition structure connecting TCB to TCC. In the same way, TCTC can also be considered as a special transition structure between TCC and SCB.

Cyclodecane. Cyclodecane represents a much more difficult conformational problem than cyclononane (see Table I and Figure 3). Only a few low-energy cyclodecane conformations have been discussed in detail.[1g,4b,4c] The symmetrical BCB form has been found to be the global minimum energy conformer by a number of force fields, and the BCB form has also been found in the crystal structure of several cyclodecane derivatives. Hendrickson has shown that the BCB form has a unique feature; namely, BCB pseudorotates with itself.[4c] Although a few other conformers have also been discussed (TCCC, BCC, CCC, TBC, TBCC), cyclodecane is considered to favor the BCB form as much as cyclohexane favors the chair form.[1g] Hendrickson[4c] and later Dale[5b] calculated interconversion barriers based on symmetry restrictions and the "torsional driving" procedure,[6] respectively. Our comprehensive conformational analysis based on the MM2 potential energy hypersurface reproduced many of the earlier calculations. The BCB conformer is the global minimum, and Figure 3 clearly shows that BCB has one single connection to the TBC form which is 4.7 kJ/mol higher in energy. Although the transition state (BTCB) exhibits a relatively high-energy barrier (26.7 kJ/mol), this is far less than the energy barrier between the chair and twist-boat forms in cyclohexane (44 kJ/mol). In fact, the BCB form does not seem to be favored more than the TBC form of cyclononane. There may be crystal packing effects that give rise to the crystals favoring the BCB form. Nonetheless, cyclodecane seems to be less mobile than cyclononane, because the cyclodecane NCI in Figure 3 exhibits mostly high-energy interconversions. *Besides the BCB form, most of the other conformers identified* previously were located. The five lowest energy conformers and their strain energies (in kJ/mol) are as follows: BCB (0), TBCC (1.8), TBC (4.7), TCCC (4.8), and BCC (6.4). The TBCC and TBC conformers were found to be very similar to those discussed by Lifson et al.[26] There is, however, an important difference, namely, that the MM2 torsion angles are symmetrical to a reflection of the ring-atom numbers (see the supplementary material) as opposed to the asymmetrical values found by Lifson. The TCCC conformer is the crown form of cyclodecane. Although the CCC conformation has been considered,[1g] CCC is, in fact, neither a minimum nor a saddle point on the MM2 potential energy hypersurface. It is instructive to note that the true BCC form is not a minimum energy conformer. BCC is, in fact, the "mirror-bridge" saddle point between the enantiomers of the slightly twisted BCC minimum energy conformer. The energy difference between the BCC saddle form and the BCC minimum form is 5.4 kJ/mol (see interconversion #1 in Table II). A further twist of the BCC form (through an asymmetrical transition state) provides the true TBCC form which is 4.6 kJ/mol lower in energy *than the twisted BCC conformer (interconversion #11).*

As far as the modes of interconversion are concerned, we have seen only K3-kayaking and double corner flapping throughout the C_6–C_9 series. Although the higher energy interconversions are dominated by the K3-kayaking mode, cyclodecane displays three new versions of the basic kayaking and flapping motions. Figure 13 shows a new flapping mode termed handle flapping ("F3") in the BCC–(BCC)–BCC interconversion (#1 in Table II; see also Figure 18). Handle flapping (almost) rigidly flaps a ring torsion angle A–B–C–D about the hinge comprised of the line AD. Interestingly, handle flapping is not associated with a unique pattern of torsion angle differences. Two handle flaps and a double corner flap are exhibited by three "mirror-bridge" MSM triads (#1, #9, and #13 in Table II). In three other interconversions (#2, #4, and #5), single corner flapping ("F2") can be seen in the same combination ("F2–F2–F22–"). Note, however, that these single corner flaps do not cross the average plane of the ring as suggested by Ōsawa.[24] Also note the alternating inward–outward pattern of flaps that seems to be a general pattern no matter which combination of flapping modes are exhibited. The TCCC–(TCCC)–TCCC interconversion between two identical conformers (subject to a rotation of the numbering system of the ring atoms) via a transition state of the same TCCC type with an axis, rather than a plane of symmetry, is an example of a different kayaking mode (see Figure 14). This mode is termed k5-kayaking, and it is different from K3-kayaking in that it involves five (A′–A–B–C–D–D′), rather than three ring bonds (A–B–C–D). Another difference is that with k5-kayaking the B–C torsion angle is nearly trans, rather than eclipsed in the transition state. The existence of an eclipsed or trans torsion angle in the transition state can be detected easily by looking at the torsion angle differences in Table II. The eclipsed case in K3-kayaking is associated with a pattern of a significant change in the B–C torsion angle and a smaller change in both the other torsion angles (A–B and C–D) that is opposite to the change in the central torsion angle ("–/++/–"). The trans case in k5-kayaking is associated with a pattern of a minor change in the B–C, A′–A, and D–D′ torsion angles and a similar but opposite change in the A–B and C–D torsion angles, respectively ("0/+/0/–/0"). Note that the other two kayaking combinations, i.e., the trans case involving three ring bonds (k3-kayaking) and the eclipsed case involving five ring bonds (k5-kayaking), also exist (see below under cycloundecane and cyclododecane).

Cycloundecane. Cycloundecane has been studied qualitatively by Dale.[5b] Only a few low-energy conformers (interconverting in a rather complex manner) were considered. Our comprehensive analysis found 17 low-energy conformers interconnected by 37 transition states (see Table I). The staircase diagram in Figure 4 reveals interesting structural details in the cycloundecane NCI. The low-energy conformers can be classified into three energy ranges. There are four conformers in the low-energy range, eight conformers in the middle range, and five conformers in the high-energy range (still <25 kJ/mol). It is instructive to note that, unlike cyclononane and cyclodecane whose global minimum can only be interconverted directly to a single conformer, cycloundecane has a global minimum that can be interconverted directly to a number of conformers. In fact, all of the middle- and high-energy conformers can be interconverted in one or two steps to one of the four lowest energy conformers. This means that the most stable conformers are located at major intersections on the NCI. It appears that cycloundecane conformers cannot be described by the chair and boat nomenclature used for describing

(26) Dunitz, J. D.; Eser, H.; Bixon, M.; Lifson, S. *Helv. Chim. Acta* **1967**, *50*, 1572–1583.

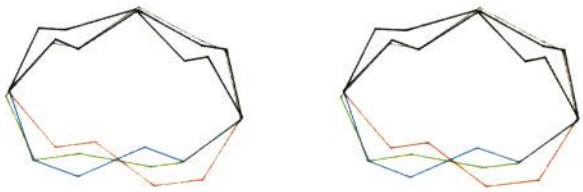

Figure 15. Cycloundecane interconversion (#19), K5-kayaking mode shown in color.

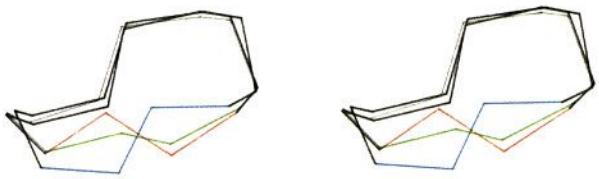

Figure 16. Cycloundecane interconversion (#36), k3-kayaking mode shown in color.

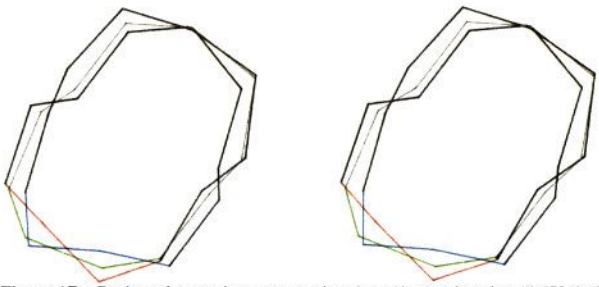

Figure 17. Cycloundecane interconversion (#10), overlapping "k5K3k5" mode (distorted K3-kayaking mode shown in color).

the smaller rings. However, cycloundecane exhibits (although in some cases less clearly) the very same simple modes of conformational interconversion found in the smaller rings. Cycloundecane also exhibits the remaining two kayaking modes of interconversion, i.e., K5-kayaking and k3-kayaking. K5-kayaking is the eclipsed version of k5-kayaking; i.e., the B–C torsion angle is nearly eclipsed, rather than trans in the transition state. The torsion angle difference pattern of K5-kayaking is "0/−/++/−/0". In the same way, k3-kayaking is the trans version of K3-kayaking with a torsion angle difference pattern "+/0/−". K5-kayaking is exhibited (along with two handle flaps) by three interconversions (#5, #19, and #21 in Table II). Figure 15 is a stereoview of the "mirror-bridge" interconversion #19. Figure 16 shows a good example of k3-kayaking in a fairly high-energy interconversion (#36). Two extremely interesting interconversions (#10 and #20) display a rare pattern of overlapped modes. In both cases, K3- and k5-kayaking modes are involved ("k5K3k5"). This combination, if not overlapped, would require at least 13 ring bonds. Figure 17 clearly shows the symmetrical overlap of both "k5" modes with the "K3" mode in the "mirror-bridge" interconversion #10. The other interconversion (#20) exhibits an asymmetrical overlap; i.e., the two "k5" modes overlap with each other and one of them overlaps with the "K3" mode. Note that, because of the overlaps (printed bold in Table II), the unique torsion angle difference patterns are destroyed.

Cyclododecane. Cyclododecane has been studied by Dale[5b] and by Anet.[27] The "square" conformer denoted by [3333] in Dale's nomenclature[28] has been found to be the global minimum energy conformer. Two other low-energy conformers, [2334] and [2343], have also been discussed. Anet considered different transition states between the [3333] and [2334] forms as well as between the [2334] and [2343] and calculated the lowest energy barriers.

(27) Anet, F. A. L.; Rawdah, T. N. *J. Am. Chem. Soc.* **1978**, *100*, 7166–7171.

(28) The numbers in the square brackets refer to the number of ring bonds between the four "corner" atoms of cyclododecane.

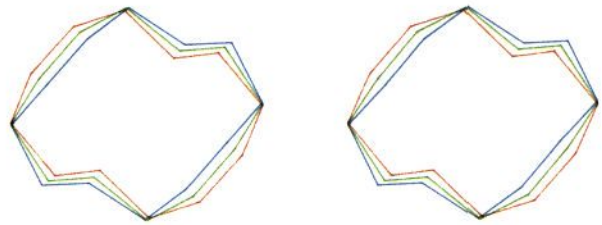

Figure 18. Cyclododecane interconversion (#2), four handle flapping modes shown in color.

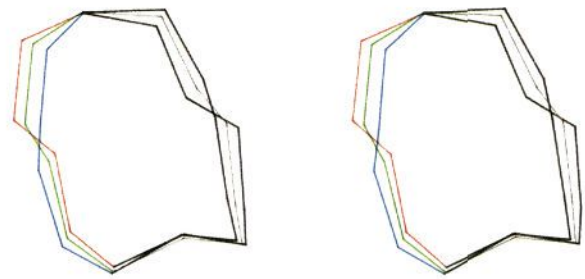

Figure 19. Cyclododecane interconversion (#15), k5-kayaking mode shown in color.

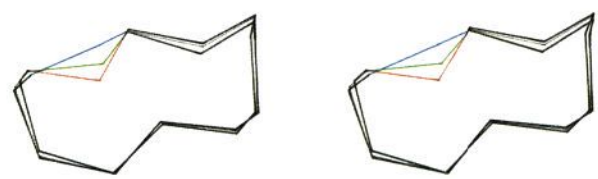

Figure 20. Cyclododecane interconversion (#7), single corner flapping mode shown in color.

Our (reasonably) comprehensive analysis found 21 low-energy minima interconnected by 36 transition states on the MM2 potential energy hypersurface (see Table I). Figure 5 shows that the [3333] conformer is a very deep global minimum. The four lowest energy conformers and their strain energies (in kJ/mol) are [3333] (0), [2334] (4.5), [1434] (7.3), and [2343] (10.3). It is instructive to note that the MM2 strain energies of [2334] and [2343] are less than those calculated by Anet[27] (6.7 and 12.1 kJ/mol, respectively). Also note that [1434] was not considered by either Dale or Anet, but later found by Saunders.[10] Figure 5 indicates only two connections to [3333]. One of them is the connection to [2334] associated with a 29.9-kJ/mol energy barrier (#11 in Table II) which is 3.1 kJ/mol less than Anet's barrier.[27] The energy barrier associated with the [2334]–[2343] interconversion is 26.7 kJ/mol (#12 in Table II) in good agreement with Anet's barrier[27] (26.4 kJ/mol). Conformational interconversions in cyclododecane exhibit all four versions of kayaking, single, and double corner flapping, and handle flapping in a variety of combinations. Similar to cycloundecane, the cyclododecane interconversions tend to be exhibited less clearly. One interconversion (#13) is associated with overlapped modes. In addition, there is one more mode of interconversion that, in fact, first appeared in two cycloundecane interconversions (#29 and #32) and also can be seen in three cyclododecane interconversions (#28, #31, and #34). This mode denoted by "Fk" seems to be a transition between single corner flapping and k3-kayaking (strongly skewed toward corner flapping). "Fk" looks like a 180° corner flap with a rather unusual transition state with the corner flapped half way through (90°) inward, rather than outward. The minima only suggest corner flapping, but the transition state is reminiscent of the transition state found in k3-kayaking modes. All of the "Fk" modes are associated with high-energy interconversions and are therefore considered to be uninteresting. Cyclododecane exhibits three aesthetically very pleasing interconversions. Figure 18 shows four symmetrical handle flaps in interconversion #2. Figure 19 shows a symmetrical double k5-kayaking mode (#15). Finally,

Figure 20 shows a perfect example of the single corner flapping (7) as suggested by Ōsawa;[24] i.e., the corner is flapped all the way to the opposite side of the plane of the ring.

Conclusions

We have demonstrated that contemporary computational methods and resources allow more to be accomplished in the field of conformational analysis than simply collecting low minimum energy conformers. It is possible to search conformational space in a more comprehensive manner, namely, to determine the complete network of conformational interconversions (NCI) within a reasonable energy window. The key is to search for saddle points on the potential energy hypersurface, rather than for minima. Although there is no simple computational technique available that converges exclusively upon saddle points, the use of a combination of the truncated Newton conjugate gradient and the full-matrix Newton–Raphson minimization methods allowed us to find saddle points at a comparable rate to finding minima. It was shown that the pair of minima associated with a particular saddle point can be found using a straightforward procedure. It was further shown that these so-called minimum-saddle-minimum (MSM) triads, each representing an individual conformational interconversion, can be fit together to solve the jigsaw puzzle of the NCI. The NCI can be visualized on a three-dimensional staircase diagram. Although the search for the NCI is obviously more computationally intensive than the traditional search for only minima, our results indicate that, using a reasonable energy window, it can be accomplished for small- to medium-ring cycloalkanes using a reasonable amount of CPU time on modern workstations.

The C_4–C_{12} cycloalkane series has been subjected to comprehensive conformational analysis with MM2 steric energies. Results derived from each NCI were in agreement with literature data on well-known conformational interconversions in the C_4–C_{12} series. Moreover, our analysis revealed that the different modes of conformational interconversion associated with the lowest barriers between minimum energy conformers display fascinating patterns of well-coordinated atomic movement. It was found that 97% of the 115 conformational interconversions in cyclohexane to cyclododecane exhibit the same basic atomic movements. Indeed, each interconversion, no matter how complex, can be decomposed into a few basic modes. There are two such basic modes termed kayaking and flapping. Kayaking involves four different modes, two of them involving three ring bonds, and the other two modes involving five ring bonds. Furthermore, both the three- and the five-bond kayaking modes have two versions, one through an eclipsed and another through a trans central torsion angle in the transition state. Flapping can be single or double corner flapping, and handle flapping. Flapping modes (in any combination) exhibit an alternating inward–outward pattern; i.e., corners and/or handles are flapped in an "in–out–in–out" fashion all around the ring. It is instructive to note that no distinction can be made between interconversions between different conformers and interconversions between identical forms or enantiomers of the same conformer in terms of modes of interconversion. Both types exhibit all basic modes of interconversion, but the interconversions between identical conformers and between enantiomers are usually more symmetrical. We believe that the kayaking and flapping modes are not artifacts of the MM2 force field. Our results suggest that kayaking and flapping are as basic to cycloalkane interconversions as torsional rotation is to *n*-alkane interconversions.

Acknowledgment. We are indebted to a reviewer for suggestions and for giving recent references to advanced saddle point search techniques.

Supplementary Material Available: Table of the MM2 steric energies and the torsion angles of all the minimum energy conformers and transition states corresponding to the MSM triads in Table II (12 pages). Ordering information is given on any current masthead page.

Nucleic Acid Dendrimers: Novel Biopolymer Structures†

Robert H. E. Hudson and Masad J. Damha*,[1]

Contribution from the Department of Chemistry, University of Toronto, Erindale College, Mississauga, Ontario, Canada L5L 1C6. *Received July 9, 1992*

Abstract: A general convergent-growth procedure for the synthesis of nucleic acid dendrimers has been developed. The synthetic strategy involves (i) the synthesis of oligonucleotides on the surface of controlled-pore glass with an automated DNA synthesizer, (ii) the introduction of the branch-point nucleoside by the coupling of two adjacent polymer-bound nucleotide chains with a tetrazole-activated adenosine 2′,3′-bis(phosphoramidite) derivative, and (iii) repetitive chain elongation and branching steps to form successive generations (G = 1–3), each with twice as many chain ends as the previous generation. Various dendrimers were constructed based on thymidine and adenosine building blocks, including an 87-unit-long dendrimer having a molecular weight of ca. 25 000 with six branch points and twelve terminal ends at the periphery of the macromolecule. Full enzymatic characterization of the dendrimers is also described.

Introduction

The past few years have been marked by research directed toward the design of highly branched macromolecules with well-defined molecular composition and constitution.[2] Since creating the first "starburst" dendrimers, the poly(amidoamines), or PAMAMs,[3] Tomalia and co-workers have synthesized a number of dendrimer families, some possessing striking similarities to anionic micelle systems.[1,4] Several other novel applications of Tomalia's "divergent-growth" approach have recently appeared, leading to dendritic poly(amidoalcohols), or "arborols",[5] polyamines,[6] poly(siloxysilanes),[7] and the micelle-like polyphenylenes[8]

† Dedicated to Professor Kelvin Kenneth Ogilvie on the occasion of his 50th birthday.

(1) Present address: Otto Maass Chemistry Building, Department of Chemistry, McGill University, Montreal, P.Q., Canada H3A 2K6.

(2) Extensive reviews of this area have appeared: (a) Tomalia, D. A.; Naylor, A. M.; Goddard, W. A., III. *Angew. Chem., Int. Ed. Engl.* **1990**, *29*, 138. (b) Tomalia, D. A.; Hedstrand, D. M.; Wilson, L. R. *Encyclopedia of Polymer Science and Engineering*, 2nd ed.; J. Wiley: New York, 1990; index volume, pp 46–92. (c) Tomalia, D. A. *New Sci.* **1991**, Nov 23, 30–34.

(3) Tomalia, D. A.; Baker, H.; Dewald, J.; Hall, M.; Kallos, G.; Martin, S.; Roeck, J.; Smith, P. *Polym. J. (Tokyo)* **1985**, *17*, 117.

(4) Gopidas, K. R.; Leheny, A. R.; Caminati, G.; Turro, N. J.; Tomalia, D. A. *J. Am. Chem. Soc.* **1991**, *113*, 7335.

0002-7863/93/1515-2119$04.00/0